Enhanced mobility of strongly localized modes in waveguide arrays by inversion of stability

Michael Öster,* Magnus Johansson,† and Anders Eriksson‡

Department of Physics and Measurement Technology (IFM), Linköping University, S-581 83 Linköping, Sweden

(Received 19 December 2002; published 9 May 2003)

A model equation governing the amplitude of the electric field in an array of coupled optical waveguides embedded in a material with Kerr nonlinearities is derived and explored. The equation is an extended discrete nonlinear Schrödinger equation with intersite nonlinearities. Attention is turned towards localized solutions and investigations are made from the viewpoint of the theory of discrete breathers (DBs). Stability analysis reveals an inversion of stability between stationary one-site and symmetric or antisymmetric two-site solutions connected to bifurcations with a pair of asymmetric intermediate DBs. The stability inversion leads to the existence of high-intensity narrow mobile solutions, which can propagate essentially radiationless. The direction and transverse velocity of the mobile solutions can be controlled by appropriate perturbations. Such solutions may have an important application for multiport switching, allowing unambiguous selection of output channel. The derived equation also supports compact DBs, which in some sense yield the best possible solutions for switching purposes.

DOI: 10.1103/PhysRevE.67.056606 PACS number(s): 42.65.Wi, 42.65.Pc, 45.05.+x, 05.45.−a

I. INTRODUCTION

In a linear directional coupler power is periodically exchanged between two adjacent waveguides due to an evanescent field overlap of the modes of the waveguides. The total power transferred is determined by the phase mismatch of the respective fields. Such a coupler can be used as a simple optical switch [1]. For multiguide directional couplers, the successive spreading of a localized pulse has been demonstrated [2]. The presence of nonlinearities drastically changes the characteristics of the couplers. Jensen derived an equation for two waveguides embedded in a nonlinear Kerr medium and showed that above a critical input a complete power exchange between the waveguides is not obtained [3]. The nonlinear transmission characteristics of the device can be utilized for the construction of optical logical gates. Similar effects of power trapping have been observed in larger arrays of waveguides, using the discrete nonlinear Schrödinger (DNLS) equation as a model equation [4,5]. Methods for controlling transverse propagating beams in both the low-intensity continuumlike domain [6] and in the high-intensity discrete domain [7] have been deviced and in the former case experimentally verified. Arrays of nonlinear waveguides thus have an important application for multiport switching.

The model derived in this paper has some important dissimilarities as compared to earlier models [5–7]. In contrast, e.g., to the recently experimentally studied structures [6], where the waveguides themselves are constructed of a nonlinear material, we have instead assumed linear waveguides embedded in a nonlinear medium as in the original model of Jensen [3]. This will tend to strengthen the effects of intersite nonlinearities as compared to the on-site nonlinearity, and will motivate an extension of the DNLS model to incorporate these effects. An approximate calculation for an array of slab waveguides shows that intersite nonlinearities can be up to the same order of magnitude as the on-site nonlinearity, provided the field penetration length is not negligible compared to the waveguide spacing. Being an extension of the ordinary DNLS model, our model is evidently more realistic as more effects are taken into account. It should though be noted that parts of the parameter regimes where the most interesting phenomena occur would mean approaching the limits of the assumptions made in the coupled-mode theory on which the derivation of the model is based. However, the range of additional phenomena appearing as compared to the DNLS model motivates investigation also into these regimes. When it comes to applications, the properties of some solutions are ideal for multiport switching, but whether they can be experimentally realized is an issue that will be left for further investigation.

The outline of our presentation is as follows. In Sec. II we derive an equation, originally derived in Ref. [8], extending the DNLS model to incorporate intersite nonlinearities and discuss some of its general properties. In Sec. III, we present some numerical results concerning linear stability of stationary solutions and demonstrate that the new equation exhibits strongly localized solutions with enhanced mobility that can be used to improve the performance of multiport switching. Finally, in Sec. IV, we will summarize our results and conclude.

II. MODEL

We will consider an array of identical optical waveguides embedded in a nonlinear Kerr material as depicted in Fig. 1. The geometry of the waveguides is quite arbitrary, but it is assumed that the fields are decaying sufficiently fast outside the waveguides to motivate only nearest-neighbor interactions. If further the electric field has a preferred direction of polarization $\hat{\boldsymbol{e}}$, like the TE and TM modes of the slab waveguide, the modes can be assumed to be real. With only a

*Electronic address: micos@ifm.liu.se

†Electronic address: mjn@ifm.liu.se

‡Present address: Swedish Defense Research Agency (FOI), P.O. Box 1165, S-581 11 Linköping, Sweden; electronic address: aneri@foi.se

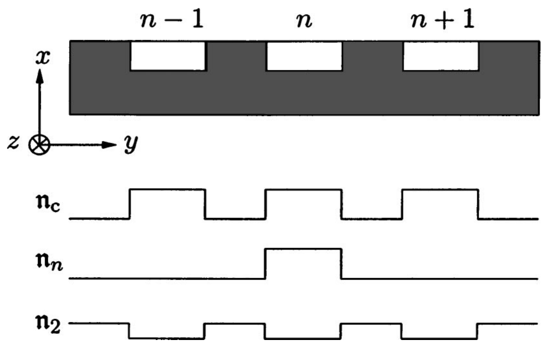

FIG. 1. An array of optical waveguides embedded in a nonlinear material. The profiles of the different refractive indices across the array are also shown. The linear refractive index of the array is $\mathfrak{n}_c$ and the linear refractive index of a single isolated waveguide is $\mathfrak{n}_n$. The Kerr index $\mathfrak{n}_2$ is zero inside the waveguides.

single identical mode present in each waveguide, the field in the nth waveguide is

$$\boldsymbol{E}_n = (\Psi_{n-1}\mathcal{E}_{n-1} + \Psi_n\mathcal{E}_n + \Psi_{n+1}\mathcal{E}_{n+1})e^{i(\beta z-\omega t)}\hat{\boldsymbol{e}}. \quad (1)$$

Ψ_n is the time-independent amplitude in waveguide n and $\mathcal{E}_n$ is the unperturbed mode, with $\mathcal{E}_{n\pm1}(\boldsymbol{r}) = \mathcal{E}_n(\boldsymbol{r}\mp\boldsymbol{d})$, $\boldsymbol{d}$ being a translation vector between adjacent waveguides. β and ω are the propagation constant (wave number) and frequency associated with the mode. The modes of the uncoupled waveguide obey an orthonormality relation and can thus be normalized. Using coupled-mode theory and expansion of the field in the orthonormal modes, the following relation can be derived [1,3]:

$$i\frac{d\Psi_n}{dz}e^{i(\beta z-\omega t)} = \frac{-1}{4\omega}\frac{\partial^2}{\partial t^2}\int\int dxdy\,\mathcal{E}_n(\boldsymbol{r})\hat{\boldsymbol{e}}\cdot\boldsymbol{P}'(\boldsymbol{r},t). \quad (2)$$

$\boldsymbol{P}'$ is the perturbing polarization arising since the waveguide is not isolated and contains both linear contributions from the adjacent waveguides and contributions from the nonlinear response of the surrounding material. From the total refractive index, $\mathfrak{n} = \mathfrak{n}_c + \mathfrak{n}_2|\boldsymbol{E}|^2$, of the array we get the total polarization, $\boldsymbol{P} = \boldsymbol{D} - \epsilon_0\boldsymbol{E} = (\mathfrak{n}^2-1)\epsilon_0\boldsymbol{E}$. For a single isolated waveguide the polarization is $\boldsymbol{P}_n = (\mathfrak{n}_n^2-1)\epsilon_0\boldsymbol{E}$ and hence the perturbing polarization is

$$\boldsymbol{P}' = \boldsymbol{P} - \boldsymbol{P}_n \approx (\mathfrak{n}_c^2 - \mathfrak{n}_n^2)\epsilon_0\boldsymbol{E} + 2\mathfrak{n}_c\mathfrak{n}_2\epsilon_0|\boldsymbol{E}|^2\boldsymbol{E}, \quad (3)$$

where only terms to first order in the Kerr index $\mathfrak{n}_2$ are kept. Plugging Eqs. (1) and (3) into Eq. (2), while sticking to the nearest-neigbor approximation due to rapidly decaying fields outside the waveguides, leads to the equation

$$\begin{aligned}-i\frac{d\Psi_n}{dz} &+ Q_1\Psi_n + Q_2(\Psi_{n-1}+\Psi_{n+1}) + 2Q_3\Psi_n|\Psi_n|^2\\ &+ 2Q_4[2\Psi_n(|\Psi_{n-1}|^2+|\Psi_{n+1}|^2) + \Psi_n^*(\Psi_{n-1}^2+\Psi_{n+1}^2)]\\ &+ 2Q_5[2|\Psi_n|^2(\Psi_{n-1}+\Psi_{n+1}) + \Psi_n^2(\Psi_{n-1}^*+\Psi_{n+1}^*)\\ &+ \Psi_{n-1}|\Psi_{n-1}|^2 + \Psi_{n+1}|\Psi_{n+1}|^2] = 0. \quad (4)\end{aligned}$$

The coupling constants Q_1–Q_5 are given by overlap integrals of the modes,

$$Q_1 = \frac{\omega\epsilon_0}{4}\int\int dxdy\,(\mathfrak{n}_c^2 - \mathfrak{n}_n^2)\mathcal{E}_n^2, \quad (5a)$$

$$Q_2 = \frac{\omega\epsilon_0}{4}\int\int dxdy(\mathfrak{n}_c^2 - \mathfrak{n}_n^2)\mathcal{E}_{n\pm1}\mathcal{E}_n, \quad (5b)$$

$$Q_3 = \frac{\omega\epsilon_0}{4}\int\int dxdy\,\mathfrak{n}_c\mathfrak{n}_2\mathcal{E}_n^4, \quad (5c)$$

$$Q_4 = \frac{\omega\epsilon_0}{4}\int\int dxdy\,\mathfrak{n}_c\mathfrak{n}_2\mathcal{E}_{n\pm1}^2\mathcal{E}_n^2, \quad (5d)$$

$$\begin{aligned}Q_5 &= \frac{\omega\epsilon_0}{4}\int\int dxdy\,\mathfrak{n}_c\mathfrak{n}_2\mathcal{E}_{n\pm1}^3\mathcal{E}_n\\ &= \frac{\omega\epsilon_0}{4}\int\int dxdy\,\mathfrak{n}_c\mathfrak{n}_2\mathcal{E}_{n\pm1}\mathcal{E}_n^3. \quad (5e)\end{aligned}$$

The derived equation governs the evolution of the electric field in an array of nonlinear waveguides. In the case $Q_4 = Q_5 = 0$ it reduces to the DNLS equation. Note also that the well-known Ablowitz-Ladik (AL) term $|\Psi_n|^2(\Psi_{n-1} + \Psi_{n+1})$ is contained in the equation. The AL equation is a special case of a fully integrable discrete version of the nonlinear Schrödinger equation [9].

To demonstrate that the constants Q_4 and Q_5 cannot always be neglected in comparison to Q_3, we make an approximate calculation for an array of slab waveguides. The integrals are to be carried out over the area between the waveguides, where the nonlinearity is present. With the separation d between the waveguides and the inverse penetration length $p = \sqrt{\beta^2 - \mathfrak{n}_c^2\omega^2\mu\epsilon_0}$, where $\mathfrak{n}_c$ is the linear part of the refractive index between the waveguides, the result is

$$\frac{Q_4}{Q_3} = \frac{pd}{\sinh(2pd)}, \quad \frac{Q_5}{Q_3} = \frac{1}{2\cosh(pd)}. \quad (6)$$

It is clear that with large penetration length or closely spaced waveguides these fractions are not negligible. However taking pd too small is not reasonable within the approximations made in the derivation of the equation, since the overlap of the modes is treated as a perturbation to an uncoupled waveguide.

General properties

Most of the properties for Eq. (4) presented here are generalizations of properties of the DNLS equation, e.g., discussed in Ref. [10]. An important feature of the equation is that it possesses quantities that are conserved as the system evolves, i.e., as the fields propagate along the array. One such quantity is the Hamiltonian [8]

$$\mathcal{H}=\mathcal{H}_1+\mathcal{H}_2+\mathcal{H}_2^*, \tag{7a}$$

$$\mathcal{H}_1=\sum_n [Q_1|\Psi_n|^2+Q_3|\Psi_n|^4], \tag{7b}$$

$$\mathcal{H}_2=\sum_n [Q_2\Psi_n\Psi_{n+1}^*+Q_4(2|\Psi_n|^2|\Psi_{n+1}|^2+\Psi_n^2\Psi_{n+1}^{*\,2}) + 2Q_5\Psi_n\Psi_{n+1}(\Psi_n^{*\,2}+\Psi_{n+1}^{*2})], \tag{7c}$$

which is real and has the symmetry $\mathcal{H}(\{\Psi_n\})=\mathcal{H}(\{\Psi_n^*\})$. Introducing the complex canonical variables $(\Psi_n, i\Psi_n^*)$, Eq. (4) can be obtained from the complex version of the Hamilton equations of motion,

$$i\frac{d\Psi_n}{dz}=\frac{\partial\mathcal{H}}{\partial\Psi_n^*}, \quad -i\frac{d\Psi_n^*}{dz}=\frac{\partial\mathcal{H}}{\partial\Psi_n}. \tag{8}$$

An important difference compared to the AL model is that there is no need for a deformed Poisson bracket to make a Hamiltonian formulation of the system [11]. We will further have a regular norm (a conserved quantity), which corresponds to conservation of (Poynting) power along the waveguides,

$$\mathcal{N}=\sum_n |\Psi_n|^2. \tag{9}$$

The conservation of norm is intimately connected to the phase invariance of Eq. (4), i.e., the fact that if $\{\Psi_n\}$ is a solution so is $\{\Psi_n e^{i\phi}\}$ for $\forall\ \phi\in\mathbb{R}$. As a consequence the constant Q_1, which connects the norm and the Hamiltonian, can be made to vanish by the simple substitution $\Psi_n\mapsto\Psi_n e^{-iQ_1 z}$. Because of the phase invariance, Eq. (4) also supports an important class of solutions with harmonically oscillating amplitude with frequency Λ, which by a transformation to a rotating frame of reference can be treated with a stationary equation. The general transformation $\Psi_n(z)=a\psi_n(bz)e^{i(b\Lambda-Q_1)z}$ will result in a rescaling of the parameters in Eq. (4) according to $Q_1\mapsto\Lambda$, $Q_2\mapsto Q_2/b=K_2$, and $Q_j\mapsto Q_j|a|^2/b=K_j$, $j=3,4,5$. An important property of the transformation is that the linear and nonlinear parameters can be scaled *independently*. To reduce the number of independent parameters we here take $b=-2Q_3|a|^2$, which scales the parameter in front of the self-interacting nonlinearity to $2K_3=-1$. For stationary ψ_n the resulting equation is

$$\Lambda\psi_n+K_2(\psi_{n-1}+\psi_{n+1})-\psi_n|\psi_n|^2+2K_4[2\psi_n(|\psi_{n-1}|^2 +|\psi_{n+1}|^2)+\psi_n^*(\psi_{n-1}^2+\psi_{n+1}^2)]+2K_5[2|\psi_n|^2(\psi_{n-1} +\psi_{n+1})+\psi_n^2(\psi_{n-1}^*+\psi_{n+1}^*)+\psi_{n-1}|\psi_{n-1}|^2 +\psi_{n+1}|\psi_{n+1}|^2]=0. \tag{10}$$

Noteworthy is also that the transformation $\psi_n\mapsto(-1)^n\psi_n$ brings a solution of Eq. (10) for the parameter values (Λ,K_2,K_4,K_5) into a solution for $(\Lambda,-K_2,K_4,-K_5)$. This reduces the part of parameter space that must be investigated to get a complete picture of the equation.

III. RESULTS

Here we will restrict our attention to localized solutions and especially discrete breathers (DBs), which are time-periodic spatially localized solutions. The time periodicity is here replaced with periodicity along the waveguides, i.e., in the variable z that plays the role of time in the Hamiltonian formulation. The existence of DBs has been rigorously proven by MacKay and Aubry [12] for Hamiltonian systems, provided that an anharmonicity condition and a nonresonance condition with linear phonons is fulfilled. The essentials are that some nonlinearity is present and that the solution has no harmonics inside the linear spectrum. The linear spectrum of Eq. (10) is $\Lambda=-2K_2\cos q$, where q is the wave number of the phonon, $\psi_n\sim e^{iqn}$. Hence phonons exist in the frequency range $|\Lambda|\leqslant 2|K_2|$.

The proof of existence is based on continuation, by virtue of the implicit function theorem, of trivial solutions from a special parameter limit of the equation, the anticontinuous limit, where the dynamics of the system is completely decoupled. For Eq. (10) we obtain this limit as $K_j=0$, $j=2,4,5$, i.e., $\Lambda\psi_n-\psi_n|\psi_n|^2=0$, with trivial solutions $\psi_n=0$ and $\psi_n=\sqrt{\Lambda}e^{i\phi}$, $\phi\in\mathbb{R}$. The idea of the proof is easily turned into an efficient numerical scheme for calculating solutions. Simply take a trivial solution in the anticontinuous limit and use it as an initial guess in an iterative Newton method following paths in parameter space [13,14].

A. Stability

Extensive calculations, covering a large portion of parameter space, have been made for the most simple solutions in the anticontinuous limit. It is convenient to identify different solutions by these initial configurations. With restriction to real solutions, each initial amplitude can be chosen from the set $\psi_n\in\{0,\pm\sqrt{\Lambda}\}$ and hence each solution can be associated with a coding sequence. Solutions originating from a configuration with one site excited with positive amplitude and the others at rest will be called one-site solutions and be denoted $(+)$, where we omit starting and trailing zeros from the notation. Similary, solutions originating from $(+,\pm)$ will be called symmetric or antisymmetric two-site solutions. Other possible one-site and two-site configurations are equivalent to these through the phase invariance. Primarily the stability properties, i.e., the behavior under small perturbations, have been investigated. To this end it is convenient to split the amplitude in real and imaginary parts, $\psi_n=x_n+iy_n$. Denote the vector of real and imaginary parts by $\psi=(\{x_n\},\{y_n\})^t$ and define through the real and imaginary parts of Eq. (10) an operator F, such that $F(\psi)=0$ if ψ is a solution. It is easily deduced that an infinitesimal nonstationary perturbation $\epsilon(z)=(\{\xi_n(z)\},\{\eta_n(z)\})^t$ to the solution ψ is governed by the equation (cf. Ref. [15])

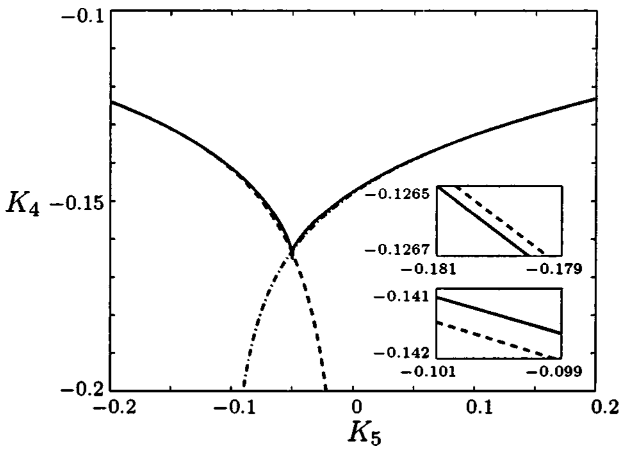

FIG. 2. Regions of stability for $(+)$ and $(+,\pm)$ solutions for $K_2=0.2$ and constant norm $\mathcal{N}=2$. The $(+)$ solutions are stable above the solid line, the $(+,+)$ solutions are stable below the dashed line, and the $(+,-)$ solutions are stable below the dash-dotted line. The boundaries almost coincide and an inversion of stability occurs between the solutions as the boundaries are crossed. The insets show a detail of the boundaries. 50 sites were used in the calculations.

$$\frac{d}{dz}\begin{pmatrix}\{\xi_n\}\\ \{\eta_n\}\end{pmatrix}=J\,F'(\psi)\begin{pmatrix}\{\xi_n\}\\ \{\eta_n\}\end{pmatrix}, \tag{11}$$

where J is orthogonal and skew symmetric and the Jacobian $F'(\psi)$ is symmetric since the system is Hamiltonian. The total matrix $JF'(\psi)$ is thus infinitesimally symplectic and must have the simultaneous eigenvalues $\pm\lambda,\pm\lambda^*$ [16]. Because of the phase invariance there is always a (double) eigenvalue at the origin. For the given solution to be linearly stable (in fact marginally stable), all eigenvalues must lie on the imaginary axis.

In Fig. 2, the stability of the different solutions is shown for $K_2=0.2$ and constant norm $\mathcal{N}=2$ in a part of parameter space. The boundaries indicate where stability of the solutions is lost. The solid line is for the $(+)$ solutions, which are stable above this line. Below the dashed line the $(+,+)$ solutions are stable and the same holds below the dash-dotted line for the $(+,-)$ solutions. All instabilities are due to eigenvalues leaving the imaginary axis at the origin along the real axis. In other regions of parameter space (mainly in the first and the second quadrant) the solutions exhibit a more complex behavior, with, for example, complex (Krein) instabilities. The interesting feature of the instabilities is that the stability boundaries of the $(+)$ and $(+,\pm)$ solutions, respectively, nearly coincide and that the stability is inverted across the boundaries. The insets show that the stability boundaries do not exactly coincide, but there is a small region of simultaneous instability for small $|K_5|$. The boundaries do intersect and for larger $|K_5|$ there will be a region of simultaneous stability. The intersection points are $(K_5,K_4)=(-0.1470,-0.1316)$ and $(0.1340,-0.1291)$, respectively. Stability inversion was first reported in Ref. [17] for a Klein-Gordon model with a double-well on-site potential and has since been verified for other models [18,19]. For DNLS-type models, a similar behavior has only recently been observed [20], but in a model with apparently little physical relevance.

In Figs. 3(a) and 3(b) the eigenvector corresponding to the eigenvalue with $\lambda>0$ (growing mode) is plotted together with the solutions at a point along the inversion boundary of the $(+)$ and $(+,+)$ solutions. The growing modes are such that one solution will grow towards something similar to the other. The behavior is the same along and nearby the entire boundary as well as along the boundary with inversion between $(+)$ and $(+,-)$ solutions. In the vicinity of the inversion boundaries we can thus have a narrow mobile DB corresponding to a repeated transformation between two stationary DBs. The phenomenon of low-radiation narrow mobile DBs has previously been observed in Klein-Gordon models and to some extent explained by the existence of a pair of intermediate DBs in the region where both solutions are unstable [18]. A closer investigation of the inversion boundaries reveals the existence of a pair of stable stationary asymmetric intermediate DBs, which we will denote (i), between the stability boundaries of the one-site and two-site

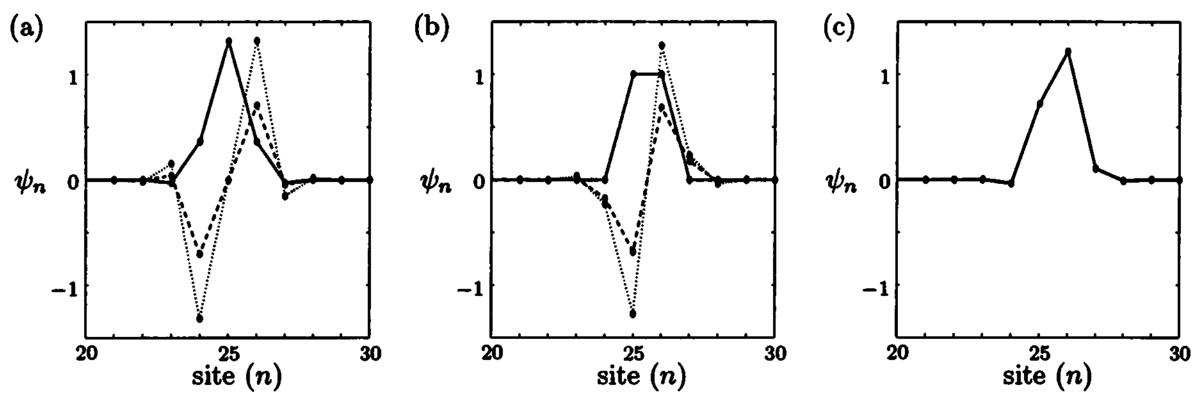

FIG. 3. The solution (solid), the real part (dashed), and the imaginary part (dotted) of the growing mode, for (a) the $(+)$ solution and (b) the $(+,+)$ solution. The imaginary part of the growing mode has been scaled by a factor of 50 to be seen better in the plot. The eigenvalues and frequencies are $\lambda=0.0600$ and $\Lambda=2.4365$ in (a) and $\lambda=0.0570$ and $\Lambda=2.4494$ in (b). The Hamiltonian of both solutions is $\mathcal{H}=-2.2494$. In (c) the stable intermediate DB is shown, with frequency $\Lambda=2.4442$ and Hamiltonian $\mathcal{H}=-2.2497$. The parameter values are $K_2=0.2$, $K_4=-0.1416$, $K_5=-0.1$ and $\mathcal{N}=2$. The number of sites is 50.

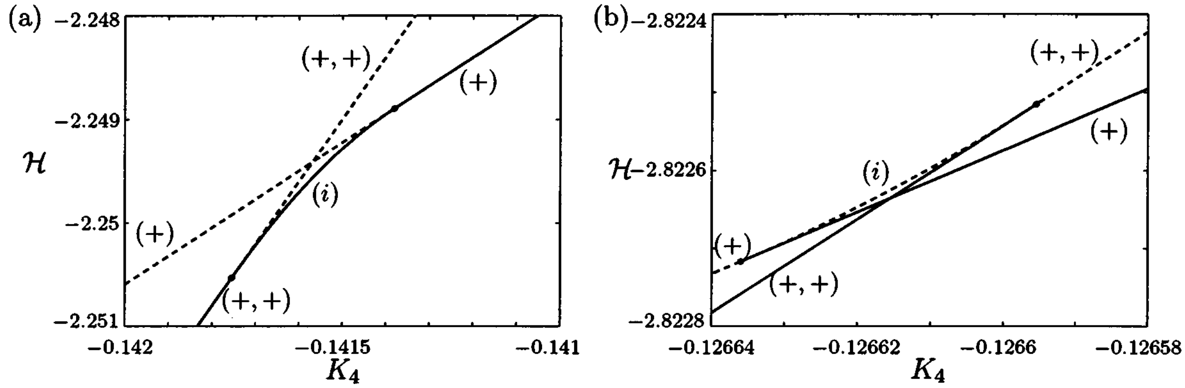

FIG. 4. Bifurcation diagrams with Hamiltonian as a function of the parameter K_4. In (a) $K_5=-0.1$ and in (b) $K_5=-0.18$. Common parameters are $K_2=0.2$ and $\mathcal{N}=2$. The different solutions and the bifurcation points are indicated in the figure. Solid (dashed) lines correspond to stable (unstable) solutions.

solutions [see Fig. 3(c)]. This intermediate solution emerges from a bifurcation at the stability boundaries as can be seen in Fig. 4. The intermediate DBs also exist in the region of *simultaneous stability* of the two stationary solutions, but it is unstable in this case. Note that the solution with the smallest value of the Hamiltonian is always stable. This observation is a rigorous result for the DNLS equation, where a ground state, i.e. a minimizer of the Hamiltonian for a given norm, is Lyapunov stable (see Ref. [21], and references therein). The ground state of the DNLS equation corresponds to a one-site solution at the anticontinuous limit and is conjectured to be essentially unique. We immediately see that neither of these is the case for Eq. (10). First, the stability of the one-site solution is lost and instead one of the two-site solutions (or the intermediate solution) minimizes the Hamiltonian and second, as a consequence, there is a boundary where the Hamiltonian is equal for two solutions [see Fig. 4(b)]. Hence equality of the Hamiltonian for the $(+)$ and $(+,\pm)$ solutions is connected to inversion of stability. This also explains why the narrow mobile DB is essentially radiationless, since the transformation connected to the motion occurs between stationary solutions of equal Hamiltonian and norm.

For application to multiport switching, it is preferrable with narrow beams to allow unambiguous selection of output channel. From this point of view it is therefore highly interesting that Eq. (10) supports *compact* DBs, i.e., solutions that are strictly zero outside an interval. The properties of compact DBs have been investigated from a mathematical viewpoint in similar models in Ref. [22], but to our knowledge this is the first report of such solutions in a physically realizable DNLS-type model. An M-site compact DB is an excitation such that $\psi_{m+j}=0$ for $j\leqslant -1$ and $j\geqslant M$ and $\psi_{m+j}\neq 0$ for $j=0,1,\ldots,M-1$. From Eq. (10) at site $n=m-1$ we then get

$$K_{\text{eff}}=K_2+2K_5|\psi_m|^2=0. \tag{12}$$

The quantity K_{eff}, when zero, describes a decoupling of sites $n<m$ from sites $n\geqslant m$ and may be taken as an approximate effective coupling between sites $m-1$ and m for small $|\psi_{m-1}|$ (and equivalently for sites $m+M-1$ and $m+M$). Note that K_2 and K_5 must have opposite signs for the existence of compact DBs. Solving for a one-site compact DB the equation at site m results in the condition $|\psi_m|^2=\Lambda$, which also will be the norm $\mathcal{N}=N$ of the solution. Hence this solution exists on the plane $K_2+2K_5N=0$ in parameter space. On either side of this plane the effective coupling, with $\text{sgn}(K_{\text{eff}})=-\text{sgn}(\psi_{m-1}/\psi_m)$, has different signs. Note that the line of zero effective coupling ($K_5=-0.05$ in Fig. 2) separates the two different inversion boundaries. Solving for a two-site compact DB gives two different real solutions, one symmetric and one antisymmetric. With the norm $\mathcal{N}=N$ we get $\psi_m=\sqrt{N/2}$ and $\psi_{m+1}=\pm\sqrt{N/2}$ together with constraints on the parameters: $K_2+K_5N=0$ and $\Lambda=\pm 3K_2-3NK_4+N/2$. For the symmetric two-site solutions the surface of existence ($K_5=-0.1$ in Fig. 2) intersects with the boundary of stability inversion. At these intersection points we can expect extremely narrow mobile solutions to exist [see also Fig. 3(b)].

B. Mobility

To investigate the dynamical properties of the DBs we integrate the nonstationary equivalent of Eq. (10) with stationary solutions as initial conditions. To induce mobility some perturbation is needed, and especially if the stationary solution is real the perturbation must be to the imaginary part of the amplitude. To see this, consider that from a Hamiltonian viewpoint the real part of the amplitude corresponds to a position variable and the imaginary part to a momentum variable. A marginal mode perturbation as described in Refs. [23,24] is a suitable perturbation. The marginal modes are the eigenvectors missing from the subspace of the two colliding eigenvalues at the stability boundary of a solution. It was proven that these grow linearly in time (z) and appeared to be the best way (very little phonon radiation) to put the DB into motion. Away from the point of instability the perturbation to a stable DB needs to have an amplitude above a threshold. A second method to induce mobility is to apply a linear phase gradient to a stationary solution, i.e., $\psi_n\mapsto\psi_n e^{ikn}$, $k\in]-\pi,\pi]$. This method was investigated,

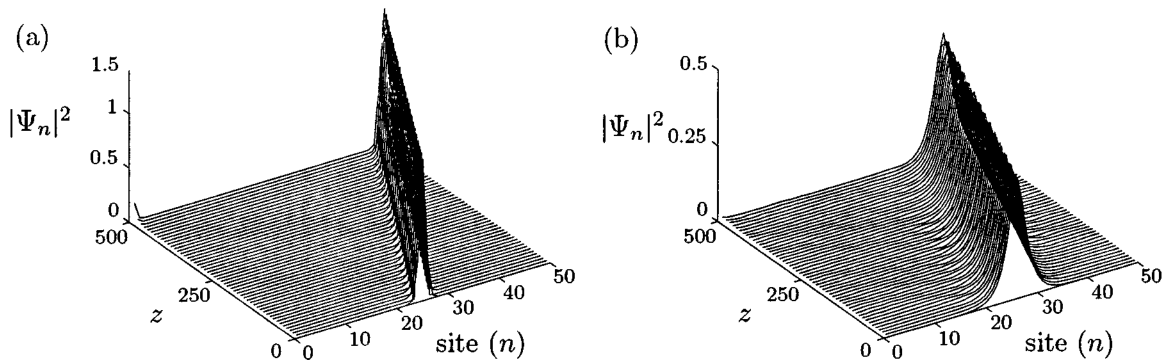

FIG. 5. (a) The solution in Fig. 3(a) with the linear phase gradient $k=0.1$. (b) A typical low-intensity mobile solution of the DNLS equation for the parameters $K_2=0.2$, $K_4=K_5=0$, $\mathcal{N}=0.47$, and $k=0.1$. The frequency is $\Lambda=0.4761$. Periodic boundary conditions are used and the accuracy of each component of the solution is 10^{-12}.

e.g., in Ref. [7] and will due to its simplicity be our primary choice for inducing mobility. The phase gradient perturbation also has the benefit of preserving the norm.

In Fig. 5, a comparison between a mobile DB of Eq. (10) and the DNLS equation is shown. The low-intensity DB of the DNLS equation is extended over several sites as opposed to the narrow high-intensity solution of Eq. (10). The latter has its analog in the DNLS equation but there high-intensity solutions have very poor mobility. The enhanced mobility for solutions of Eq. (10) may be explained by the presence of stability inversion. Since the resulting moving DB is essentially radiationless it can, in principle, propagate indefinitely. Simulations for up to $z\sim10^5$ show no noticeable change in the solution. Some radiation is inevitable due to the perturbation and numerical inaccuracies. For the solutions of Fig. 5 with periodic boundary conditions, the excitations will propagate against a background of $|\psi_n|^2\sim10^{-7}$–10^{-8} in (a) and $|\psi_n|^2\sim10^{-5}$–10^{-6} in (b). A more relevant measure for switching purposes is the contrast of the output defined by $C=|\psi_{n_e}(L)|^2/[|\psi_{n_e-1}(L)|^2+|\psi_{n_e}(L)|^2+|\psi_{n_e+1}(L)|^2]$, where n_e is the site with maximum power and $z=L$ is the total length of the waveguides. Obviously the solution in (a) has a higher contrast, $0.50\leqslant C\leqslant0.87$, depending on L, as compared to $0.41\leqslant C\leqslant0.45$ for the DNLS solution. 0.5 is the best lower bound that can be achieved for propagating high-intensity solutions, since this occurs when the stationary two-site solution involved is compact. For switching purposes a high contrast is ideal. The upper bound can be improved by considering solutions where the planes of existence of the compact one-site and two-site solutions are closer. In Ref. [7] better lower bounds on C are achieved by displacing a trapped high-intensity DNLS solution an integer number of waveguides by a collision with a low-intensity transverse propagating solution.

The strength of the applied phase gradient can be used to control the motion of the mobile DB. Although the norm is preserved by the perturbation the Hamiltonian will increase, giving excess energy (not actual energy, since $\mathcal{H}$ is not the energy of the system) to the stationary solution. Since the perturbation is symmetry breaking, the energy will be carried away in either direction, depending on the sign of k, as kinetic energy of the mobile DB. A larger phase gradient will result in a higher transverse velocity, v ($[v]$ is sites per waveguide length). For small k it roughly holds that $k\propto v$

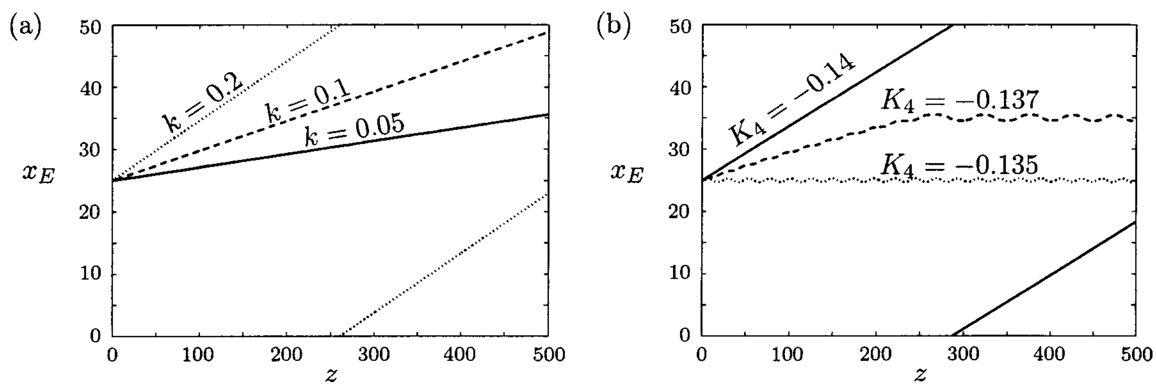

FIG. 6. (a) Displacement of the center of energy for different phase gradients with the one-site solution in Fig. 3(a) as initial solution. Note that k is proportional to the slope in the figure, i.e., the transverse velocity. (b) Center of energy for fixed phase gradient, $k=0.2$, and different initial one-site solutions in the vicinity of the inversion boundary. Common parameters are $K_2=0.2$, $K_5=-0.1$, and $\mathcal{N}=2$. At $K_4=-0.135$ the perturbation is below the threshold, at $K_4=-0.137$ it is near the threshold, and at $K_4=-0.14$ it is above the threshold.

[see Fig. 6(a)]. The constant of proportionality depends on the initial stationary solution, since the same phase gradient will give different changes to the Hamiltonian, $\Delta\mathcal{H}$. A more general relation for small k, supported by numerical simulations, is $\Delta\mathcal{H}\propto v^2$, which indicates that the excess energy indeed is carried away as kinetic energy. Hence an effective mass m^* of the mobile DB can be defined by the relation $\Delta\mathcal{H}=m^*v^2/2$ (see also Refs. [23,24]).

In the vicinity of the inversion boundary a stable solution can be put into motion if the perturbation is large enough, i.e., there is a threshold to surmount to induce mobility. If the size of the perturbation is below the threshold, the DB will just oscillate without moving. For larger perturbations the resulting moving DB will still show good mobility. In Fig. 6(b), the displacement of the center of energy is shown for solutions with varying distance from the inversion boundary. Note the different behavior when the perturbation is below, above, or approximately at the threshold. The motions are not entirely radiationless, not even for the relatively large perturbation, and hence the mobile solutions will eventually get trapped. When perturbing an unstable solution there is no threshold and the mobility remains very good, although some radiation will still escape.

IV. CONCLUSIONS

A model equation for arrays of nonlinear coupled optical waveguides has been derived and examined in the context of discrete breathers. The phase invariance of the equation led us to investigate stationary solutions and especially their stability properties, revealing an inversion of stability between symmetric or antisymmetric two-site DBs and one-site DBs. Narrow solutions with enhanced mobility exist at the inversion boundaries corresponding to a transformation between the stationary solutions, via an asymmetric intermediate DB emerging from a bifurcation at the stability boundaries.

Our work was primarily motivated by the desire to obtain highly localized beams with extremely good mobility, which could be used for switching purposes in waveguide arrays. Thus, we found that taking into account additional nonlinear terms, which normally are neglected in the standard DNLS treatment, could lead to a drastic enhancement of the mobility of narrow solutions. In our model, such effects may arise when the field penetration length is not negligible compared to the waveguide spacing. Furthermore, even compact solutions corresponding to complete beam localization in one single (or several) waveguide(s) could be found when the Kerr index of the nonlinear material, or equivalently, the intensity of the field, is large [cf. Eq. (12)].

A priori, we believe that our assumptions are not unrealistic, and we should note that in parts of the parameter regime where the interesting phenomena appear, the intersite nonlinear interactions are still considerably smaller than the on-site nonlinearity. However, whether this regime is experimentally available is an issue that needs further investigation.

Leaving aside the nonlinear optics application, our results are interesting from several other points of view. First, we have presented what we believe to be the first example of strictly compact solutions in a DNLS-like model which might be experimentally realizable. (Our model was not included in the class of models previously shown [22] to possess compact solutions.) In fact, the full complexity of the model studied here is not at all necessary for obtaining compact solutions; the only necessary ingredients are the simultaneous presence of the on-site nonlinearity and the last two terms in the Q_5 part of Eq. (4). Second, to our knowledge our model is also the first example of a realistic DNLS-like model where inversion of stability between site-centered and bond-centered solutions has been observed and analyzed. In this aspect, the crucial ingredient was shown to be the presence of the Q_4 part of Eq. (4) (as inversion of stability was found also for $Q_5=0$). Also, to the best of our knowledge, the scenario illustrated in Fig. 4(b) with a regime of *simultaneous stability* for site-centered and bond-centered breathers has not been observed in any earlier studied model.

Although we believe that this is the first time that our model (4) has been considered and analyzed in its full generality, it is interesting to note that for a particular choice of parameter values it coincides with models previously derived in completely different contexts. Namely, for $Q_4=Q_5=Q_3/2$, it is equivalent to an equation derived in Ref. [25] as a rotating-wave approximation to a Fermi-Pasta-Ulam chain. Likewise, for the same parameter values it is a subclass of a model proposed in Ref. [26] to describe energy transport in an exciton-phonon (or vibron-phonon) coupled system modeling α-helical proteins, taking into account both acoustic and optic phonons. In both these papers, the equation is analyzed through soliton perturbation theory from the integrable Ablowitz-Ladik model, and the tendency of the off-diagonal nonlinear terms to enhance mobility compared to the pure on-site DNLS model is noted. Note, however, that the parameter regime of main interest in our work is quite far from these special values.

As a final remark, we point out that in analyzing the stability regimes and bifurcation diagrams we have compared solutions continued at constant norm rather than at constant frequency, which is often done. In particular, this allows for an interpretation of the difference in the Hamiltonian of the breathers as a "Peierls-Nabarro-like" energy barrier that should be minimized in order to optimize the mobility. A similar comparison between breathers at constant frequency would not allow for such an interpretation, since the breather frequency generally changes in the movement. Still, we have analyzed also the counterparts to the stability diagrams for continuation at constant frequency; these results will appear elsewhere [27].

ACKNOWLEDGMENTS

We thank V. V. Konotop for providing us with preprints of Ref. [22] and related work prior to their publication. M.J. acknowledges support from the Swedish Research Council.

[1] A. Yariv, *Optical Electronics in Modern Communications*, 5th ed. (Oxford University Press, New York, 1997).
[2] S. Somekh, E. Garmire, A. Yariv, H.L. Garvin, and R.G. Hunsperger, Appl. Phys. Lett. **22**, 46 (1973).
[3] S.M. Jensen, IEEE J. Quantum Electron. **18**, 1580 (1982).
[4] L.J. Bernstein, Opt. Commun. **94**, 406 (1992).
[5] D.N. Christodoulides and R.I. Joseph, Opt. Lett. **13**, 794 (1988).
[6] H.S. Eisenberg, Y. Silberberg, R. Morandotti, A.R. Boyd, and J.S. Aitchison, Phys. Rev. Lett. **81**, 3383 (1998).
[7] O. Bang and P.D. Miller, Phys. Scr. T **67**, 26 (1996).
[8] A. Eriksson, Master's thesis LiU-IFM-Fysik-Ex-468, Linköping University, 1995 (unpublished).
[9] M.J. Ablowitz and J.F. Ladik, J. Math. Phys. **16**, 598 (1975); **17**, 1011 (1976).
[10] J.C. Eilbeck, P.S. Lomdahl, and A.C. Scott, Physica D **16**, 318 (1985).
[11] A. Scott, *Nonlinear Science* (Oxford University Press, Oxford, 1999).
[12] R.S. MacKay and S. Aubry, Nonlinearity **7**, 1623 (1994).
[13] J.C. Eilbeck, P.S. Lomdahl, and A.C. Scott, Phys. Rev. B **30**, 4703 (1984).
[14] J.L. Marín and S. Aubry, Nonlinearity **9**, 1501 (1996).
[15] J. Carr and J.C. Eilbeck, Phys. Lett. **109A**, 201 (1985).
[16] C. Robinson, *Dynamical Systems: Stability, Symbolic Dynamics and Chaos*, 2nd ed. (CRC Press, Boca Raton, 1999).
[17] D.K. Campbell and M. Peyrard, in *CHAOS–Soviet American Perspectives on Nonlinear Science*, edited by D.K. Campbell (AIP, New York, 1990), p. 305.
[18] T. Cretegny, Ph.D. thesis (in French), École Normale Supérieure de Lyon, 1998 (unpublished).
[19] J.L. Marín, S. Aubry, and L.M. Floría, Physica D **113**, 283 (1998).
[20] K. Kundu, J. Phys. A **35**, 8109 (2002).
[21] M.I. Weinstein, Nonlinearity **12**, 673 (1999).
[22] P.G. Kevrekidis and V.V. Konotop, Phys. Rev. E **65**, 066614 (2002).
[23] S. Aubry and T. Cretegny, Physica D **119**, 34 (1998).
[24] D. Chen, S. Aubry, and G.P. Tsironis, Phys. Rev. Lett. **77**, 4776 (1996).
[25] Ch. Claude, Yu.S. Kivshar, O. Kluth, and K.H. Spatschek, Phys. Rev. B **47**, 14 228 (1993).
[26] K. Kundu, Phys. Rev. E **61**, 5839 (2000).
[27] M. Öster and M. Johansson, in *Proceedings of the Conference on Localization and Energy Transfer in Nonlinear Systems, San Lorenzo de El Escorial, Madrid, Spain, 2002,* edited by L. Vázquez, M. P. Zorzano, and R. MacKay (World Scientific, Singapore, in press).